Impact of SSTA in the East Indian Ocean on the Frequency of Northwest Pacific Tropical Cyclones: A Regional Atmospheric Model Study

RUIFEN ZHAN

Laboratory of Typhoon Forecast Technique, Shanghai Typhoon Institute, China Meteorological Administration, Shanghai, China

YUQING WANG

International Pacific Research Center, and Department of Meteorology, School of Ocean and Earth Science and Technology, University of Hawaii at Manoa, Honolulu, Hawaii

CHUN-CHIEH WU

Department of Atmospheric Sciences, National Taiwan University, Taipei, Taiwan

(Manuscript received 11 December 2010, in final form 2 May 2011)

ABSTRACT

The impact of the sea surface temperature anomaly (SSTA) in the East Indian Ocean (EIO) on the tropical cyclone (TC) frequency over the western North Pacific (WNP) and the involved physical mechanisms are examined using the International Pacific Research Center (IPRC) Regional Atmospheric Model (iRAM) driven by the reanalysis and the observed SSTs. The model reproduces generally quite realistic climatic features of the WNP TC activity, including the interannual variability of the WNP TC genesis frequency, the geographical distributions of TC genesis and frequency of occurrence. In particular, the model reproduces the observed statistical (negatively correlated) relationship between the WNP TC frequency and the EIO SSTA, as recently studied by Zhan et al.

The experiments with artificially imposed SSTA in the EIO in the year 2004 with normal EIO SST and WNP TC activity confirm that the EIO SSTA does affect the TC genesis frequency in the entire genesis region over the WNP by significantly modulating both the western Pacific summer monsoon and the equatorial Kelvin wave activity over the western Pacific, two major large-scale dynamical controls of TC genesis over the WNP. Additional sensitivity experiments are performed for two extreme years: one (1994) with the highest and one (1998) with the lowest TC annual frequencies in the studied period. The results reveal that after the EIO SSTAs in the two extreme years are removed, the TC frequency in 1998 is close to the climatological mean, while the excessive TCs in 1994 are still simulated. The model results suggest that the warm EIO might be a major factor contributing to the unusually few TCs formed over the WNP in 1998, but the cold EIO seemed to contribute little to the excessive WNP TCs in 1994.

1. Introduction

The El Niño–Southern Oscillation (ENSO), the strongest interannual climate fluctuation on the earth (e.g., Philander 1990), has been recognized as the most important large-scale environmental factor controlling the interannual variability of tropical cyclone (TC) activity over the western North Pacific (WNP; e.g., Chan 2000; Wang and Chan 2002; Chia and Ropelewski 2002). It is considered as one of the main predictors in statistically based seasonal forecast models for the WNP TC activity (Chan et al. 1998; Chan and Liu 2001). Previous studies have revealed that ENSO greatly modulates the mean location of TC genesis and TC intensity over the WNP (e.g., Wang and Chan 2002; Camargo and Sobel 2005; Zhan et al. 2011). The impact of ENSO, however, does not seem to be robust on any aspect of the WNP TC activity. In particular, the correlation between ENSO and the annual genesis frequency of the WNP TCs is not statistically significant (Ramage and Hori 1981; Lander 1994; Wang and Chan 2002; Chen et al. 2006). Therefore,

Corresponding author address: Dr. Yuqing Wang, IPRC/SOEST, University of Hawaii at Manoa, Rm. Post 409G, 1680 East-West Rd., Honolulu, HI 96822.
E-mail: yuqing@hawaii.edu

DOI: 10.1175/JCLI-D-10-05014.1

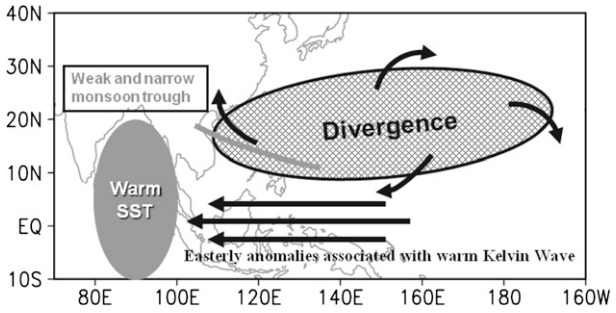

FIG. 1. Schematic diagram showing the response of the atmospheric fields over the WNP to the EIO warming. Warm SSTA over the EIO reduces the land–sea thermal contrast to the north and weakens the East Asian and WNP summer monsoon. It also excites a warm equatorial Kelvin wave to the east with low-level easterly anomalies with negative surface pressure anomalies near the equator over the WNP. Consequently, positive surface pressure anomalies accompanied with anticyclonic divergent circulation occur in the tropics off the equator over the WNP TC genesis region, suppressing the TC formation over the WNP.

what factors control the interannual variability of the WNP TC genesis frequency still remains an issue.

More recently, several observational studies have brought new perspectives to this important issue (Du et al. 2011; Zhan et al. 2011). The Indian Ocean (IO) sea surface temperature anomaly (SSTA) has been documented to play a vital role in affecting TC genesis frequency over the WNP. Du et al. (2011) found a sharp decrease in TC number in summer (July–September) due to the effect of the prolonged SST warming over the IO following strong El Niño events and showed that the increase in vertical wind shear is responsible for the changes in the observed WNP TC frequency. Zhan et al. (2011) focused on the effect of East Indian Ocean (EIO) SSTA and noted that the WNP TC genesis frequency is considerably higher in the years when the EIO is cold than it is warm in spring and summer. In the work by Zhan et al. (2011), two mechanisms by which the EIO SSTA affects the WNP TC genesis frequency have been highlighted, as shown schematically in Fig. 1. The first mechanism is related to the effect of the EIO SSTA on the East Asian and WNP summer monsoon. Warm (cold) EIO SSTA implies reduced (enhanced) land–sea thermal contrast, leading to weaker (stronger) than normal East Asian and WNP summer monsoon and its associated monsoon trough, thus suppressing (promoting) TC genesis over the WNP. The second mechanism is associated with the equatorial Kelvin wave dynamics as identified by Xie et al. (2009). The EIO warm (cold) SSTA can excite a warm (cold) equatorial Kelvin wave to the east over the WNP, lowering (increasing) the surface pressure in the equatorial region and leading to anomalous anticyclonic (cyclonic) vorticity and divergence (convergence) in the tropics off the equator in the WNP TC genesis region. These would result in anomalous descending (ascending) motion and a dry (wet) middle troposphere, thus suppressing (promoting) convective activities and TC genesis over the WNP.

A major limitation of the observational analysis lies in the difficulty of identifying dominant controlling factors from different arguments. In addition, the reliability of historical data for TCs is also a great concern (Knutson et al. 2010). It is anticipated that numerical modeling can provide additional assessment for the mechanisms revealed based on the observational analysis. Factors controlling the interannual variability of TC frequency can be analyzed in a dynamically consistent way based on model outputs. In this regard, numerical simulations with a credible dynamical model and observational analysis with reliable data are complementary. In recent years, there have been a number of studies focusing on the dynamical simulations of TC activity using global climate models (GCMs; e.g., Knutson et al. 1998; Vitart and Anderson 2001; Murakami et al. 2011) or high-resolution regional climate models (RCMs; e.g., Stowasser et al. 2007; Camargo et al. 2007; Knutson et al. 2007, 2008).

Because of constraints in spatial resolution and computation costs, GCMs are used to simulate large-scale circulations and provide the lateral boundary conditions to drive RCMs. Stowasser et al. (2007), for example, discussed the influence of global warming on the climatology of TCs in the WNP basin using the International Pacific Research Center (IPRC) RCM (IPRC-RegCM, now named iRAM) forced by SST and lateral boundary conditions from a coupled GCM. To assess the suitability for an RCM to be used for future climate change assessment in a given basin, the model is generally evaluated first by using reanalysis data as the driving fields, which provide both initial and lateral boundary conditions as input for RCM. Stowasser et al. (2007) showed that the iRAM simulated reasonably well the climatology of both large-scale fields and annual TC number over the WNP in the 10-yr period from 1991 to 2000 without using any large-scale nudging in the model interior. This is in sharp contrast to a study by Knutson et al. (2007), who showed that in order to reproduce the observed multidecadal increase and interannual variations of hurricane activity in the North Atlantic basin by a high-resolution RCM, they had to optimally nudge the large-scale components of winds, temperature, and moisture in their model interior toward the driving fields, which were obtained from the National Centers for Environmental Prediction–National Center for Atmospheric Research (NCEP–NCAR) reanalysis. The strong sensitivity of their model-simulated TC frequency to the nudging coefficient implies that the

model has considerable discrepancies in reproducing the large-scale circulation for the North Atlantic basin.

In addition to applications to the climate change assessment, RCMs have also been utilized for climate process studies to understand physical mechanisms that shape the observed climate features in various regions (see a review by Wang et al. 2004a). In the present study, we are interested in understanding the relationship between the EIO SSTA and the WNP TC activity by using a dynamical model, as a follow-up effort after Zhan et al. (2011). We choose iRAM since its credibility in reproducing main features of TC activity over the WNP has been demonstrated by Stowasser et al. (2007). As in Stowasser et al. (2007) and Knutson et al. (2007), we drive iRAM using the observed SST and NCEP–NCAR reanalysis. Since we use a much larger model domain in this study to include the EIO than that in Stowasser et al. (2007), we will first reevaluate the model's performance in simulating the observed interannual variability of the WNP TC genesis frequency for the period 1990–2008, and then use the model to investigate the impact of EIO SSTA with well-designed sensitivity experiments. We will show that without the use of any large-scale nudging, iRAM can reproduce the observed interannual variability of TC genesis frequency over the WNP reasonably well. More importantly, the model shows promising skills in simulating the response of the WNP TC genesis frequency to the EIO SSTA and the associated physical mechanisms as revealed based on observations by Zhan et al. (2011).

The rest of the paper is organized as follows. Section 2 provides a brief description of the model, experimental design, and the datasets. The results from a control simulation and a series of sensitivity experiments are presented in sections 3 and 4, respectively. The main conclusions are drawn in the last section together with a brief discussion.

2. Methodology

a. Model description

The dynamical model used in this study is the regional climate model iRAM developed at IPRC, at the University of Hawaii at Manoa (Wang et al. 2003). The model uses hydrostatic, primitive equations in spherical coordinates with sigma (pressure normalized by surface pressure) as the vertical coordinate. The model equations are solved with a fourth-order conservative horizontal finite-differencing scheme on an unstaggered longitude–latitude grid system. The time integration is performed using a leapfrog scheme with intermittent application of an Euler backward scheme. The model physics include the cloud microphysics scheme of Wang (2001); a mass flux scheme for subgrid shallow convection, midlevel convection, and deep convection developed by Tiedtke (1989) with some modifications outlined in Wang et al. (2003, 2004b, 2007); the radiation package developed by Edwards and Slingo (1996) and further improved by Sun and Rikus (1999); the Biosphere–Atmosphere–Transfer Scheme (BATS) developed by Dickinson et al. (1993) for land surface processes; a modified Monin–Obukhov similarity scheme for flux calculations at the ocean surface; and a nonlocal E–ε turbulence closure scheme for subgrid-scale vertical mixing (Langland and Liou 1996), which was modified to include the effect of cloud buoyancy production of turbulence kinetic energy (Wang 1999). A one-way nesting is used to update the model time integration in a buffer zone near the lateral boundaries within which the model prognostic variables are nudged to reanalysis data with an exponential nudging coefficient proposed by Giorgi et al. (1993) and later modified by Liang et al. (2001). The buffer zone is 5° in extent. More details of the model can be found in Wang et al. (2003, 2004b, 2007).

The version of the model used in this study has 28 vertical levels with relatively higher resolution in the planetary boundary layer. The lowest model level is roughly 35 m above the surface. The model domain covers the EIO and the WNP, extending from 15°S–56.5°N to 70°E–160°W with a grid spacing of 0.5° in both zonal and meridional directions, as shown in Fig. 2a. Such a resolution is still too coarse to represent the observed structure and intensity of real TCs. For example, the minimum central sea level pressure of 940 hPa and the maximum surface wind of 46 m s^{-1} are the most intense storm simulated in the control simulation, compared with 910 hPa and 65 m s^{-1} in observations in June–October for the period 1990–2008. The deficiency of the underestimated TC intensity in the model is also shared by a number of other RCMs (Camargo et al. 2007; Knutson et al. 2007). Since we focus on the frequency and location of TC genesis in this study, the underestimation of storm intensity is not a big issue. As we will show in section 3, the model with 0.5° grid spacing employed here can simulate the interannual variability of frequency and the location of WNP TC genesis reasonably well.

b. Experimental design

The initial and lateral boundary conditions for iRAM in all experiments are obtained from the NCEP–NCAR reanalysis (Kalnay et al. 1996), available at 2.5° × 2.5° horizontal resolution with 17 vertical pressure levels at 6-h intervals. They are interpolated onto the model grids by cubic spline interpolation in the horizontal and linear interpolation in both the vertical and time. The simulations

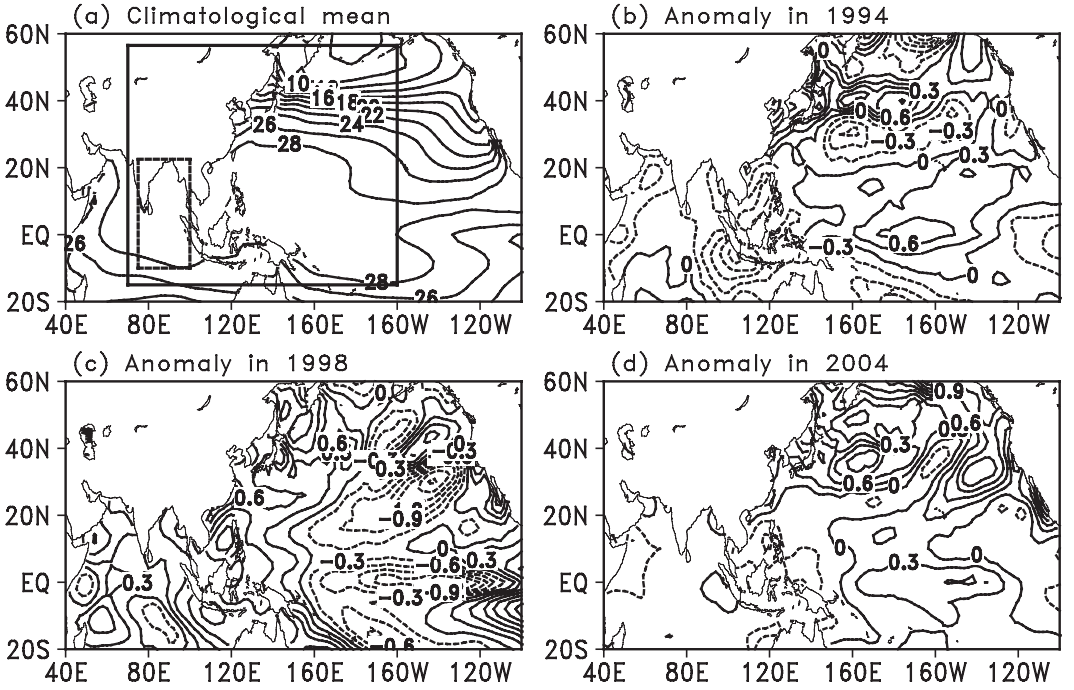

FIG. 2. (a) Climatological mean SST (°C) and mean SSTA (°C) in the period June–October (b) 1994, (c) 1998, and (d) 2004 in observations. In (a), the solid box indicates the domain used for the RCM simulations, and the dashed one indicates the EIO.

described here are initialized at 0000 UTC 27 May of each year, and integrated through the end of October for the period 1990–2008. The 6-hourly output from each experiment is analyzed for the typhoon season during June–October, as defined in Zhan et al. (2011). The main difference in these experiments is the use of either the Reynolds weekly SST at 1° × 1° horizontal resolution (Reynolds et al. 2002) or with some modifications to the SST field.

1) Control simulation (CTRL): The Reynolds weekly SST was used to perform simulations for 19 typhoon seasons (1990–2008). The simulation was designed to verify the model's ability in reproducing the TC statistics of the observed WNP TC activity.
2) CS_2004 and WS_2004 runs: These two sensitivity experiments were carried out for 2004, a normal TC year with both TC number and EIO SSTA close to their climatological mean as shown in Fig. 2d. The CS_2004 run was identical to the control run except that 1°C was subtracted from the SST in the EIO (10°S–22.5°N, 75°–100°E), while in the WS_2004 run 1°C was added to the SST in the EIO.
3) CLM_1994 and CLM_1998 runs: During 19 typhoon seasons from 1990 to 2008, the WNP had 33 TCs in 1994, being the busiest TC season and only 10 TCs in 1998, being the quietest TC season. The observed SST anomalies in Figs. 2b,c show that the EIO was colder than normal in the summer of 1994 and warmer than normal in the summer of 1998. These are consistent with the relationship between the WNP TC frequency and the EIO SSTA detected by Zhan et al. (2011). These two years were chosen to discuss the impact of the EIO SSTA on the extreme years over the WNP. In both CLM_1994 and CLM_1998 runs, the weekly SSTs in the EIO used in the CTRL run were replaced by the climatological weekly SSTs constructed from the Reynolds weekly SST during 1990–2008, while the SSTs in other regions remained unchanged.

c. *Criteria for identifying TCs*

The method for detecting and tracking the model TCs is similar to that used in earlier studies by Nguyen and Walsh (2001) and Stowasser et al. (2007) with some modifications for our model resolution and domain. With 6-hourly model outputs, the following criteria must be satisfied for a system to be identified as a tropical storm in our simulations:

1) There must be a relative vorticity local maximum at 850 hPa exceeding 5×10^{-5} s^{-1}.
2) There must be a local minimum in sea level pressure within a distance of 4° latitude or longitude from the

vorticity maximum; this minimum pressure is defined as the center of the model storm.
3) The azimuthal mean tangential wind speed at 850 hPa must be higher than at 300 hPa.
4) The closest local maximum in temperature averaged between 500 and 200 hPa is distinguishable and is defined as the center of the warm core. The distance between the center of the warm core and the center of the storm must not exceed 2.5° latitudes. From the center of the warm core the temperature must decrease by at least 0.5°C in all directions within a distance of 7.5°.
5) The storm must form at latitudes south of 35°N and at longitudes east of 100°E.

To be considered as a model tropical storm trajectory, a storm must last at least 1 day and have a maximum wind speed of over 17 m s^{-1} at the lowest model level during at least 1 day (not necessarily consecutive). For each storm snapshot, a check is performed to see if there are storms during the following 6-h period within a distance of 300 km south of 25°N or 600 km north of 25°N. If there are none, the trajectory is considered to have stopped. If there are some, the closest storm is designated as belonging to the same trajectory as the initial storm. Cases satisfying all these criteria are referred to as TCs in this study.

d. Observational TC data

Following Zhan et al. (2011), the best-track TC data (6-hourly position and intensity) obtained from Shanghai Typhoon Institute of China Meteorological Administration (CMA) are used to evaluate the model simulations. There are also best-track datasets available from the Joint Typhoon Warning Center (JTWC) and the Regional Specialized Meteorological Center of the Japan Meteorological Agency (JMA). They show different typhoon intensities, but consistent interannual variability in TC genesis frequency since 1980 (Zhan et al. 2011). The CMA best-track data started in 1949, but the period 1990–2008 is used in this study to verify the model simulations for the same period. In addition, we only considered TCs that reached at least the tropical storm (TS) intensity (with maximum sustained wind speed $V_{max} \geq$ 17 m s^{-1}).

3. Control simulations

Stowasser et al. (2007) concluded that iRAM can reproduce reasonably well the climatology of the observed TC behavior and the associated large-scale fields. In this section, we will focus on the model's performance in simulating the interannual variability of TC genesis frequency over the WNP and in reproducing the observed relationship between the WNP TC frequency and the EIO SSTA.

We begin with evaluation of the simulated frequency and geographical distribution of WNP TCs. During 1980–2008, mean 20 TCs formed over the WNP in each typhoon season. The simulated seasonal mean total number is about 18, slightly lower than the observation. The frequencies of TC genesis and occurrence in the 19 typhoon seasons are calculated in each 5° longitude by 5° latitude grid box, as shown in Fig. 3. The TC genesis location in the CTRL simulations resembles that observed (Figs. 3a,b), with a maximum band of TC formation between 5° and 25°N where the monsoon trough exists and two local maxima: one in the South China Sea (SCS), and one around 130°E. However, the TC genesis frequencies near the two local maxima are slightly lower in the model than in the observation and the TC genesis locations east of the Philippines are remarkably shifted northward in the model.

When a TC passes a grid box, TC occurrence in this grid box is counted once. The maximum frequency of occurrence is used to infer the prevailing tracks. The geographical distribution of the TC occurrence frequency is simulated quite well (Figs. 3c,d). Both the model and the observation show a maximum band between 15°–25°N and 105°–150°E. However, the model shows a local maximum over the SCS, which does not appear in its observed counterpart. In addition, the frequency of occurrence north of 28°N in the observation is considerably underestimated in the model, notably over Korea and Japan and east of Japan's main island. These discrepancies are similar to those reported in Stowasser et al. (2007), and might be related to the less TC frequency simulated in September and October and the deficiency in the TC detection algorithm, which excludes the extratropical transitions of any tropical systems since any detected systems with a warm core more than 2.5° away from the surface center are excluded from the tropical storms. Nevertheless, these discrepancies are not a serious problem in this study since our focus is on the TC genesis frequency, which is reasonably simulated in the model as discussed above.

Figure 4 shows the monthly mean WNP TC numbers during the typhoon season averaged for 1990–2008 in the CTRL simulation and the observation. The month-to-month variation in the WNP TC genesis frequency is well reproduced by the model. Although the simulated frequencies in September and October are respectively about 25% and 50% lower than those observed, the model simulates an increase from June to August, a maximum in August, and a decrease from August to October, in agreement with the observed results.

Figure 5 shows the time series of the WNP TC numbers in the typhoon season for simulations and observations

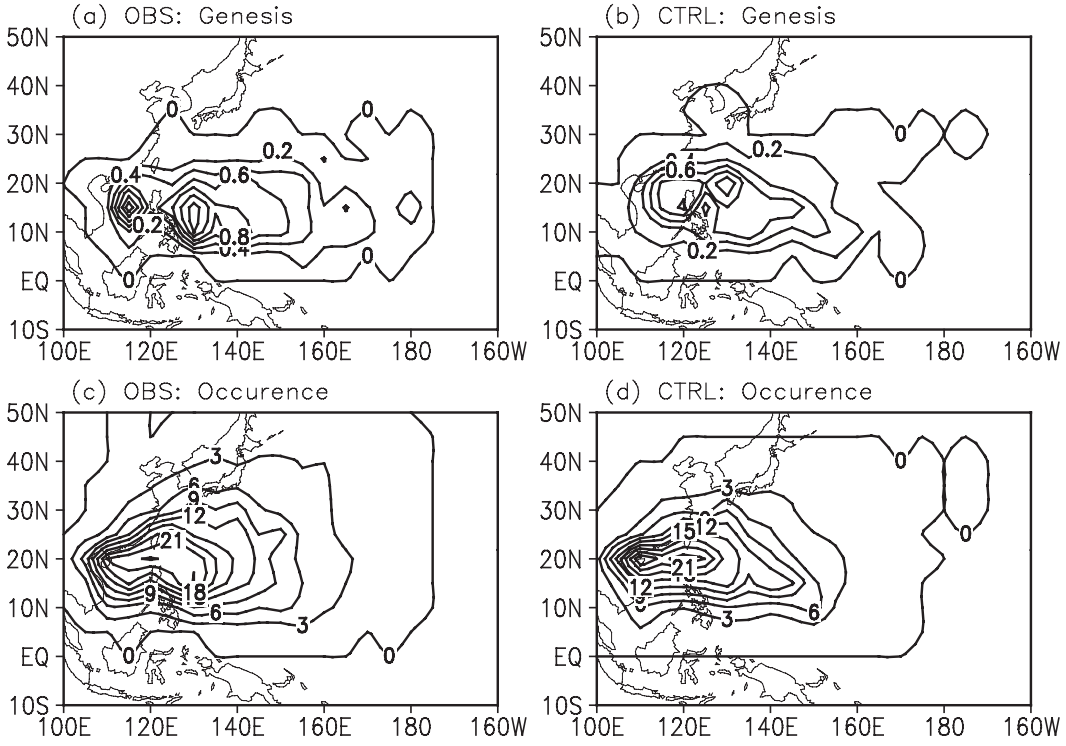

FIG. 3. Observed frequencies of TC (a) genesis and (c) occurrence in each 5° latitude × 5° longitude grid box. (b),(d) The corresponding frequencies from the model simulation.

from 1990 to 2008. There is a good correspondence between the simulated and observed time series, with a correlation coefficient of 0.75 at 99% confidence level based on the Student's *t* test and a root-mean-square error of 1.3. The least squares linear trends from 1990 to 2008 for simulations and observations are also presented in Fig. 5. A decrease in the WNP TC frequency since 1990 is evident in both observations and simulations. After subtracting the trends of the two series, a high correlation still remains with a coefficient of 0.65 at the 99% confidence level. These results suggest that the model has substantial skill in reproducing the observed variability and the trend of WNP TC genesis frequency. The promising simulation can be attributed to the model's good skills in capturing the large-scale environment and the triggering mechanisms for TC genesis over the WNP as indicated by Stowasser et al. (2007), although the model resolution of 0.5° is too coarse to resolve all aspects of TCs. Note that the model underestimates the TC frequencies after 2000. Differences between observations and simulations for 2000 and 2001 are particularly distinct. This leads to fewer seasonal mean TC number for the 19 typhoon seasons in our CTRL simulation than in the observation (18 in the simulation vs 20 in the observation) and a faster linear decreasing trend in the total TC number during the typhoon season in the simulation than in the observation. The reason for the underestimation of TC frequency after 2000 remains unknown and will be a topic for future studies.

To evaluate whether the model has skills in reproducing the response of the observed TC frequency to SSTA over the EIO, Fig. 5 also represents time series of the observed EIO SSTA in summer. Similar to the observed TC frequency, the simulated WNP TC frequency shows a clear negative correlation with the EIO summer SSTA, with a correlation coefficient of −0.62 at the 99% confidence level based on the Student's *t* test. After the

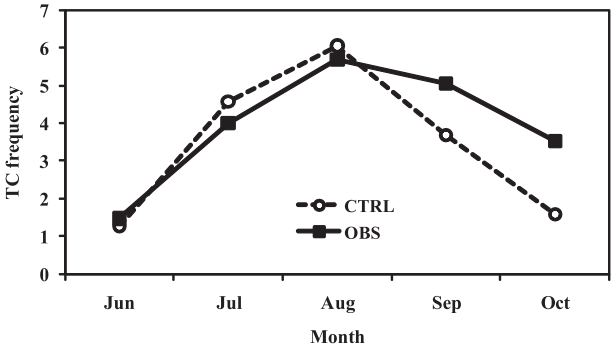

FIG. 4. Seasonal variations of simulated (dashed line) and observed (solid line) WNP TC numbers.

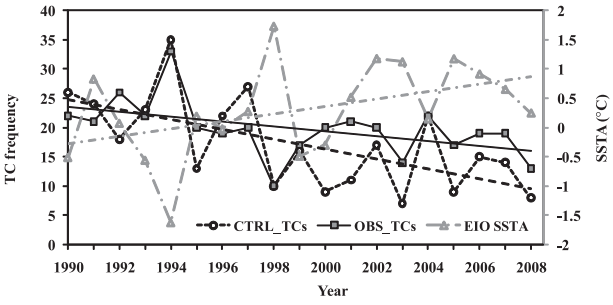

FIG. 5. Interannual variations of simulated (dashed line and hollow circle) and observed (solid line and box) WNP TC numbers for the typhoon season, and normalized summer EIO SSTA (dotted line and hollow triangle) during 1990–2008. Least squares best-fit linear trends are represented by the corresponding unmarked lines.

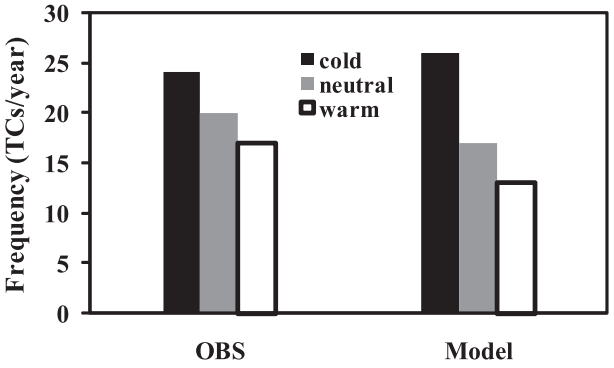

FIG. 6. Frequency of WNP TC genesis during EIO SST cold years (black), neutral years (gray), and warm years (hollow). Results are shown for observations and simulations for 1990–2008. EIO SST cold years include 1990, 1993, 1994, and 1999. EIO SST warm years include 1991, 1998, 2001, 2003, 2005, 2006, and 2007. The remaining years are neutral. Cold (warm) year is defined with SSTA ≤ -0.5 (SSTA ≥ 0.5) standard deviation.

linear trends of two time series are removed, the correlation coefficient still reaches -0.48 at the 95% confidence level. Furthermore, we examine the differences in the WNP TC genesis frequency in different classifications, namely cold, neutral, and warm years, of the EIO in the CTRL simulations. Based on the observed summer SSTAs over the EIO during 1990–2008, we define cold (warm) EIO years as years in which the summer SSTA ≤ -0.5 (SSTA ≥ 0.5) standard deviation and the remaining years as neutral. Zhan et al. (2011) showed that the WNP TC genesis frequency of a particular year is higher when the EIO in summer is cold than when it is warm. Consistent with their results, the observation does show higher (lower) TC genesis frequency over the WNP in the cold (warm) EIO years than in the neutral years (Fig. 6). Our CTRL simulation successfully reproduces this overall tendency except that the model somewhat magnifies the difference in the WNP TC genesis frequency between cold and warm EIO years, that is, more TCs form in cold EIO years and fewer TCs in warm EIO years compared with the observations (Fig. 6). The results suggest that the model has significant skill in simulating the observed relationship between the EIO SSTA and the WNP TC frequency in the studied period and can be used as a tool to assess contributions of the EIO SSTA to the interannual variability of TC genesis over the WNP, as will be discussed in the next section.

4. Sensitivity experiments

To examine to what degree the EIO SSTA affects the WNP TC genesis frequency and to understand the involved physical mechanisms proposed by Zhan et al. (2011), we choose one normal year (2004) and two extreme years (1994 and 1998) to conduct four sensitivity experiments in this section as outlined in section 2b.

a. Experiments in a normal year (2004)

1) TC FREQUENCY

Figure 7a shows the observed frequency and positions of TC formation over the WNP during the typhoon season of 2004. In this season, 22 TCs formed over the WNP, close to the multiyear mean of 20 discussed in section 3. Most of them formed in the east of the Philippines and only a few formed over the SCS. Surprisingly, the CTRL simulation (Fig. 7b) produces the same TC number and a consistent trend of the geographical distribution except for an evident westward shift.

Figures 7c,d show the WNP TC genesis frequency and locations from the CS_2004 and WS_2004 runs, respectively. A prominent feature is a sharp change in TC number. The TC number produced in the WS_2004 run with 1°C warmer over the EIO than in the CTRL run is 15, while 32 TCs are simulated in the CS_2004 run with 1°C colder over the EIO than in the CTRL run. The TC number in the former run thus is decreased by 32% while in the latter run is increased by 46% compared with that in the CTRL run as shown in Table 1. Another distinct feature is that the decrease or increase in the WNP TC frequency seems to occur anywhere in the entire basin. These results suggest that the EIO SSTA may not affect the TC genesis location significantly but affects the frequency remarkably in the entire genesis region over the WNP as indicated by Zhan et al. (2011) based on observational analysis.

2) LARGE-SCALE FIELDS

Figure 8 shows 850-hPa wind fields in the typhoon season of 2004 for the model simulation and the NCEP–NCAR reanalysis. In the reanalysis (Fig. 8a), the southwesterly

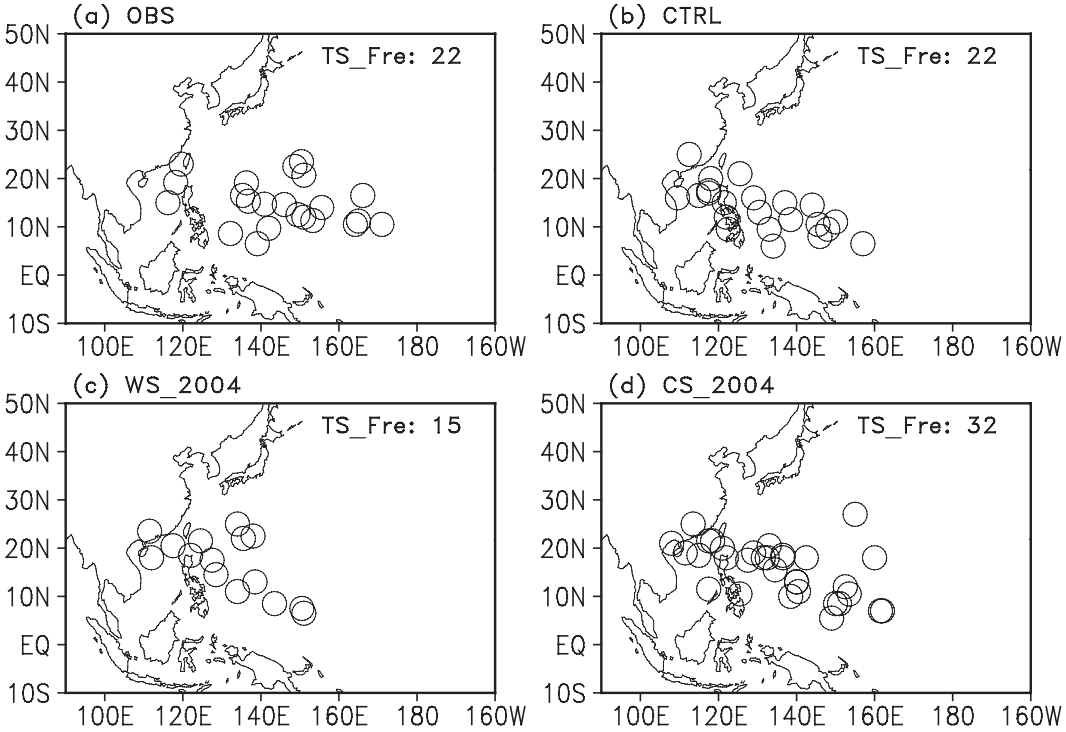

FIG. 7. Positions of TC genesis over the WNP from (a) the observations, (b) the CTRL experiment, (c) the WS_2004 experiment, and (d) the CS_2004 experiment for the typhoon season of 2004. The numbers in the top-right corner indicate the TC genesis frequencies over the WNP.

monsoonal flow prevails from the Indian Ocean to the WNP. The monsoon trough over the WNP is located over the SCS and east of the Philippines, accompanied by the strong WNP subtropical high to the northeast. The CTRL run (Fig. 8b) reproduces these main features well, but the monsoon trough over the SCS in the simulation is too strong. When SST over the EIO is lowered by 1°C in the CS_2004 run, the southwesterly monsoonal flow over the WNP intensifies, and the monsoon trough over the SCS and east of the Philippines deepens and extends eastward and northward (Fig. 8d). This is because the cold EIO SSTA implies an increased land–sea thermal contrast, leading to stronger SCS and WNP summer monsoon, more favorable for the WNP TC genesis. In contrast, the WS_2004 run with 1°C warmer in the EIO than the CTRL run produces remarkably weaker southwesterly monsoonal flow over the WNP due to the decreased land–sea thermal contrast, as well as a weaker monsoon trough, suggesting an unfavorable environment for TC genesis in the WNP basin.

The impact of the EIO SSTA can be better examined in the difference fields for the typhoon season between the WS_2004 and the CS_2004 runs. Following Zhan et al. (2011), we show the differences in 850-hPa winds (Fig. 9a), deep-layer mean tropospheric temperature (Fig. 9b), 850-hPa vorticity (Fig. 9c), 900-hPa divergence (Fig. 9d), sea level pressure (Fig. 9e), and 500-hPa vertical p velocity (Fig. 9f). The differences between the WS_2004 run and the CS_2004 run are in good agreement with the results in Zhan et al. (2011). As shown in the deep tropospheric temperature (Fig. 9b), the warm EIO excites a warm equatorial Kelvin wave in the troposphere with warm temperature anomalies in the equatorial region to the east over the western Pacific, which lowers the surface pressure (Fig. 9e) and produces anomalous low-level convergence in the equatorial region (Fig. 9d). An immediate response to the above equatorial anomalies is the divergence and subsidence in the tropics off the equator, leading to an increase in surface pressure, a decrease in relative vorticity (Fig. 9c) and an anomalous anticyclonic circulation (Fig. 9a) in the main WNP TC genesis region. Du et al. (2011) found that the increase

TABLE 1. TC frequencies over the WNP in the typhoon season from the observation and model simulations in 2004 and the changes (relative to that in the CTRL run in percentage) of TC frequencies in the two sensitivity experiments.

	Obs	CTRL run	WS_2004 run	CS_2004 run
TC frequency	22	22	15	32
Relative change (%)	—	—	−32%	+46%

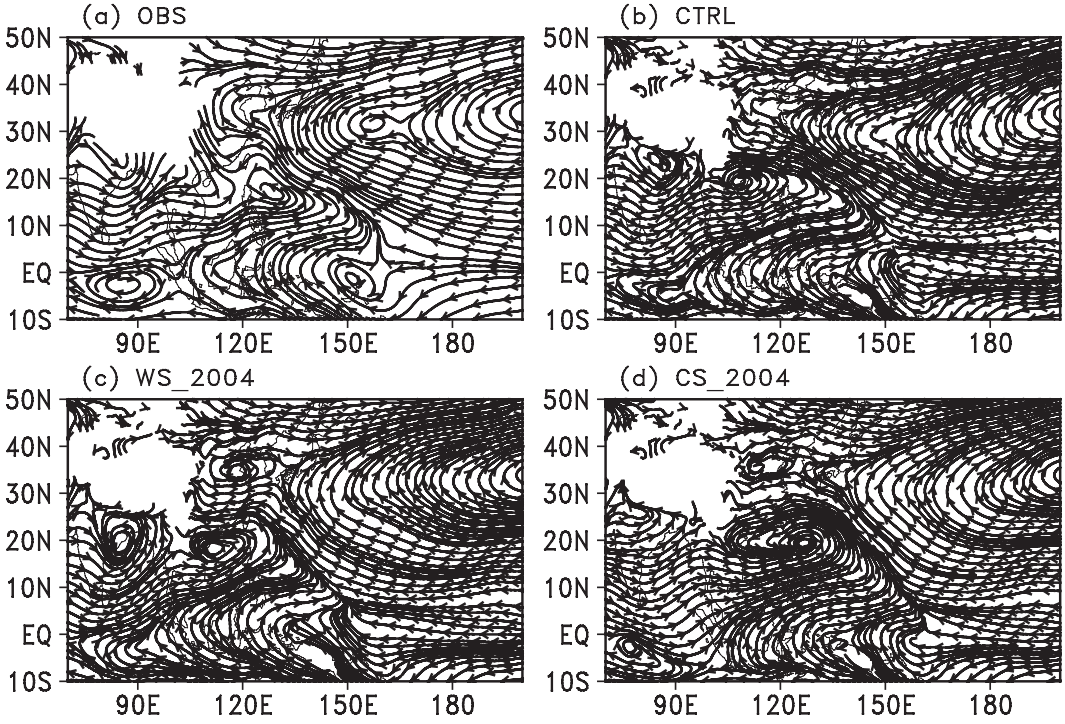

FIG. 8. 850-hPa wind fields averaged in the typhoon season of 2004 from (a) the NCEP–NCAR reanalysis, (b) the CTRL experiment, (c) the WS_2004 experiment, and (d) the CS_2004 experiment.

or decrease in vertical wind shear associated with the EIO SSTA is also responsible for the changes in the observed WNP TC frequency. We thus examined vertical shear of zonal wind between 850 and 200 hPa and specific humidity at 600 hPa (Figs. 9g,h). Consistent with Du et al. (2011), the warm Kelvin wave associated with the warm EIO SSTA triggers westerly vertical shear anomalies over most of the tropical WNP basin (Fig. 9g). The westerly vertical shear anomalies east of 150°E increase the magnitude of vertical shear in that region. However, the westerly vertical shear anomalies north 15°N and west of 150°E shift the low shear region southward, although such anomalies decrease the magnitude of vertical shear over the south SCS. It suppresses TC genesis over the north SCS, showing somewhat different result from Du et al. (2011). In addition, Fig. 9h shows that the warm EIO produces a drier midtroposphere compared to the cold EIO in most of the WNP, especially in the main TC genesis region east of the Philippines. These dynamical conditions account for fewer TCs in the WS_2004 run and more TCs simulated in the CS_2004 run. The above results confirm the mechanisms proposed by Zhan et al. (2011) that the EIO SSTA highly modulates TC formation over the WNP through affecting both the equatorial atmospheric wave dynamics and the East Asian and WNP summer monsoon circulation.

b. Experiments in two extreme years (1994 and 1998)

Results from our sensitivity experiments in a normal year discussed above strongly support the causal relationship between the WNP TC and the EIO SSTA. A question arises as to whether the EIO SSTA can explain and is responsible for the unusual TC frequencies over the WNP in extreme years. This is addressed by conducting two additional sensitivity experiments for the year 1994 with the most TCs (CLM_1994) and the year 1998 with the fewest TCs (CLM_1998) over the WNP. As mentioned in section 2b, in both CLM_1994 and CLM_1998 runs, the weekly SSTs in the EIO used in the CTRL run were replaced by climatological weekly SSTs.

Before conducting the sensitivity experiments, the basic environmental conditions in these two years are briefly reviewed. In the summer and fall of 1994, an El Niño event was developing. Figure 2b shows positive SST anomalies in the central and eastern equatorial Pacific. In contrast, La Niña condition was developing during the second half of 1998 after the warm event in 1997/98. As shown in Cheung (2004), in the summer of 1994 the SCS and WNP summer monsoon was intensified and low vertical wind shear region extended to central Pacific that enabled TC formations throughout the basin, while in the summer of

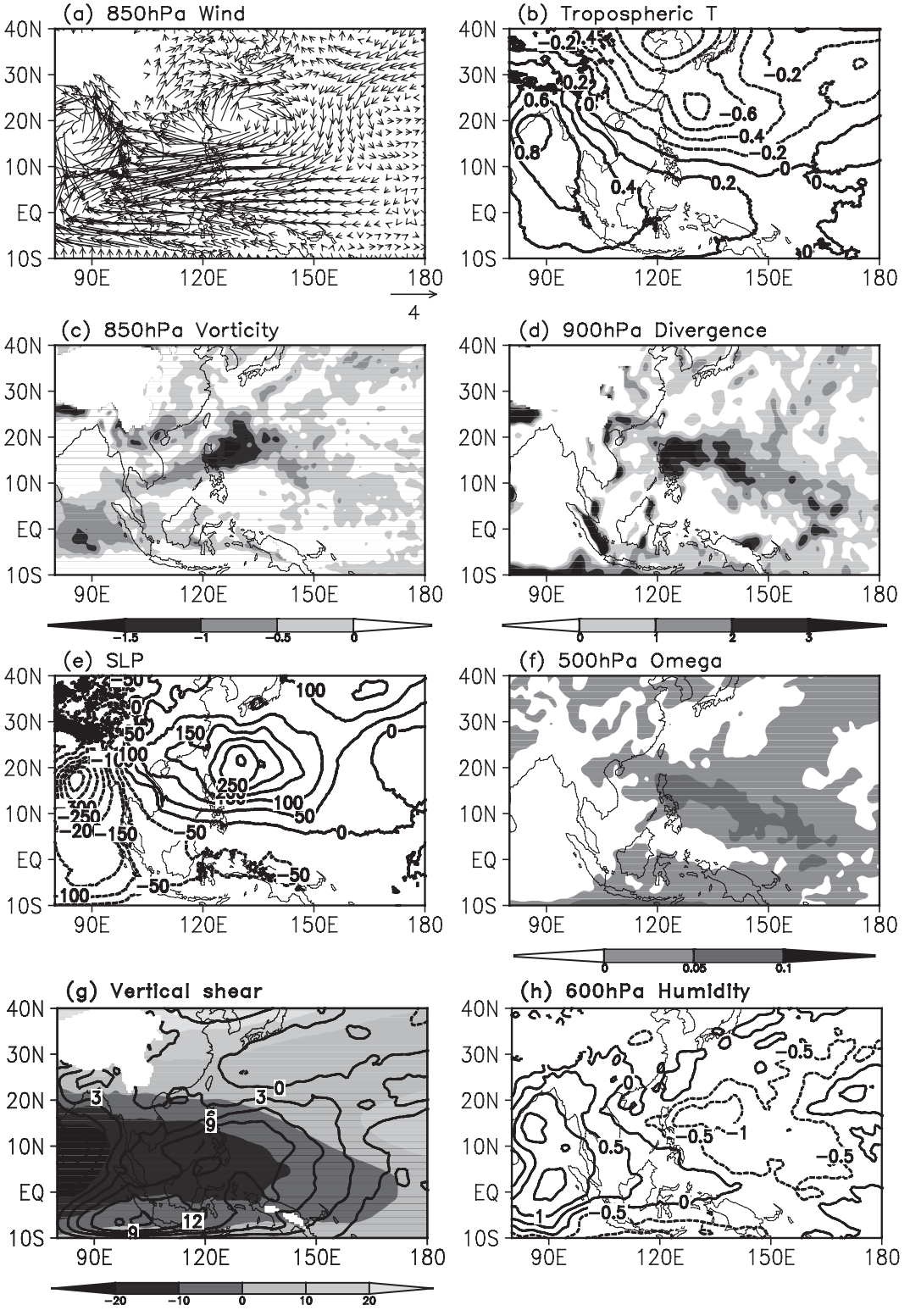

FIG. 9. The simulated differences between the WS_2004 run and the CS_2004 run in (a) 850-hPa winds (m s^{-1}), (b) deep-layer mean tropospheric temperature (°C), (c) 850-hPa vorticity (10^{-5} s^{-1}), (d) 900-hPa divergence (10^{-6} s^{-1}), (e) sea level pressure (Pa), (f) 500-hPa vertical p velocity (Pa s^{-1}), (g) zonal wind vertical shear (contour, m s^{-1}) between 200 and 850 hPa, and (h) 600-hPa specific humidity (10^{-3} kg kg^{-1}). Shading in Fig. 9g indicates zonal wind vertical shear in the WS_2004 run.

TABLE 2. TC frequencies over the WNP basin and three subregions for the typhoon season in the observations and models in 1994 and 1998.

Years	1994	1998
Subregions	B/W/M/E*	B/W/M/E*
Obs	33/7/11/15	10/2/8/0
CTRL run	35/3/18/14	10/4/5/1
CLM run	31/3/11/17	16/6/8/2

* B: the whole WNP basin, W: the west WNP west of 125°E, M: the central WNP between 125° and 145°E, and E: the east WNP east of 145°E.

1998 the SCS and WNP summer monsoon was weak and the low-shear region was restricted west of about 150°E. Generally, during La Niña developing years, the TC genesis frequency has no obvious difference from that during El Niño developing years except that the mean location of TC genesis shifts westward (Wang and Chan 2002; Zhan et al. 2011). However, the year of 1998 is also a decay year of a strong El Niño event. Following strong El Niño, a robust warming occurred over the EIO and persisted through summer as shown in Fig. 2c, which is unfavorable for TC genesis (Du et al. 2011). In the summer of 1994, the EIO was colder than normal. Thus, the EIO SSTA might contribute to the unusual TC genesis frequency in these two years. In the following, we will test this hypothesis by conducting several sensitivity experiments.

Table 2 shows the TC frequencies over the WNP basin for the typhoon season in the observation and the model simulations. The observation shows 33 and 10 TCs in the typhoon season of 1994 and 1998, respectively. Our CTRL simulation produces 35 TCs in 1994 and 10 TCs in 1998, very close to the observed. Camargo et al. (2007) tried to reproduce the WNP TC activity in these two years by using the Max-Plank Institute GCM ECHAM4.5 and the NCEP regional spectral model (RSM), but failed. They found that the ECHAM4.5 did reproduce few TCs over the WNP in 1998 but did not produce enough in 1994, while the nested RSM did not reproduce more TCs in 1994 than in 1998. Here, our CTRL run well reproduces the total TC frequencies in both 1994 and 1998. Table 2 compares the TC numbers from the observation, the CTRL run, and the climatogical SST runs for the two extreme years. With the SSTs in the EIO replaced by the climatological mean SSTs, the TC numbers in both extreme years show a tendency toward the climatological mean value, namely, less TCs in CLM_1994 and more TCs in CLM_1998 than those in the CTRL run, suggesting that the EIO SSTA does contribute to the TC genesis over the WNP in the two extreme years. However, the extent of the contribution of the EIO SSTA varies greatly. The TC number in 1998 increases from 10 in the CTRL run to 16 in the CLM_1998 run, an increase of 60% after the warm SSTA in summer over the EIO is removed, very close to the model climatological mean of 18. This suggests that the warm EIO is a major factor leading to the unusually few TCs formed over the WNP in 1998. In contrast, the TC number in 1994 is reduced by only about 10% of the observed, still excessive compared to the climatological mean, suggesting little effect of the EIO SSTA on TC genesis in this extreme typhoon season. Actually, we also performed two additional experiments with increases in SST by 1° and 2°C, respectively, in the EIO compared to the SST used in the CTRL run. The experiment with SSTs 1°C warmer in the EIO led to almost the same result as in CLM_1994 run, with 30 TCs over the WNP. The 1 with SSTs 2°C warmer over the EIO produced 22 TCs over the WNP, the closest number to the climatological mean in the observation. However, as shown in Fig. 2b, the SSTAs in most of the EIO region in 1994 are 1°C colder than those in the climatological mean. A 2°C increase in the EIO SSTA should lead to much fewer TCs than the climatological mean according to the EIO SSTA–WNP TC relationship, such as 10 TCs over the WNP in 1998 with SSTA less than 1°C warmer in the EIO (Fig. 2c).

The TC genesis locations over the WNP in these two extreme years for the observations and the simulations are compared in Fig. 10. In the observations, the WNP TCs formed in a wide band between 10° and 25°N from the SCS to the date line in 1994, while in 1998 TCs tended to form mostly west of 150°E. Our CTRL simulations reproduce the distribution of the genesis latitude band in 1994 and the feature of concentrated genesis locations in 1998 in addition to the well-simulated TC numbers as indicated above. However, the zonal extent of the TC formation region in 1994 in the observation (Fig. 10a) is not simulated well (Fig. 10b), and a northward shift in 1998 are also present in the CTRL simulations (Figs. 10d,e). When the SSTAs in the EIO are removed in the two sensitivity experiments, the TC genesis location in 1994 extends eastward and the increase in TC genesis in 1998 tends to occur in the whole basin. According to the longitudinal distribution of correlations of the WNP TC frequency with the summer EIO SSTA index shown in Zhan et al. (2011), the correlation between the EIO SSTA and the TC frequency over the WNP has a sharp decrease to the west of 125°E and to the east of 145°E. To further examine the response of the simulated TC genesis frequency to the EIO SSTA in the two years, we divided the WNP into three subregions: the west region west of 125°E, the central region between 125° and 145°E, and the east region east of 145°E. The TC frequencies in the three subregions from the observation and the model simulations are also given in Table 2. As indicated above, the bias in TC genesis location between the

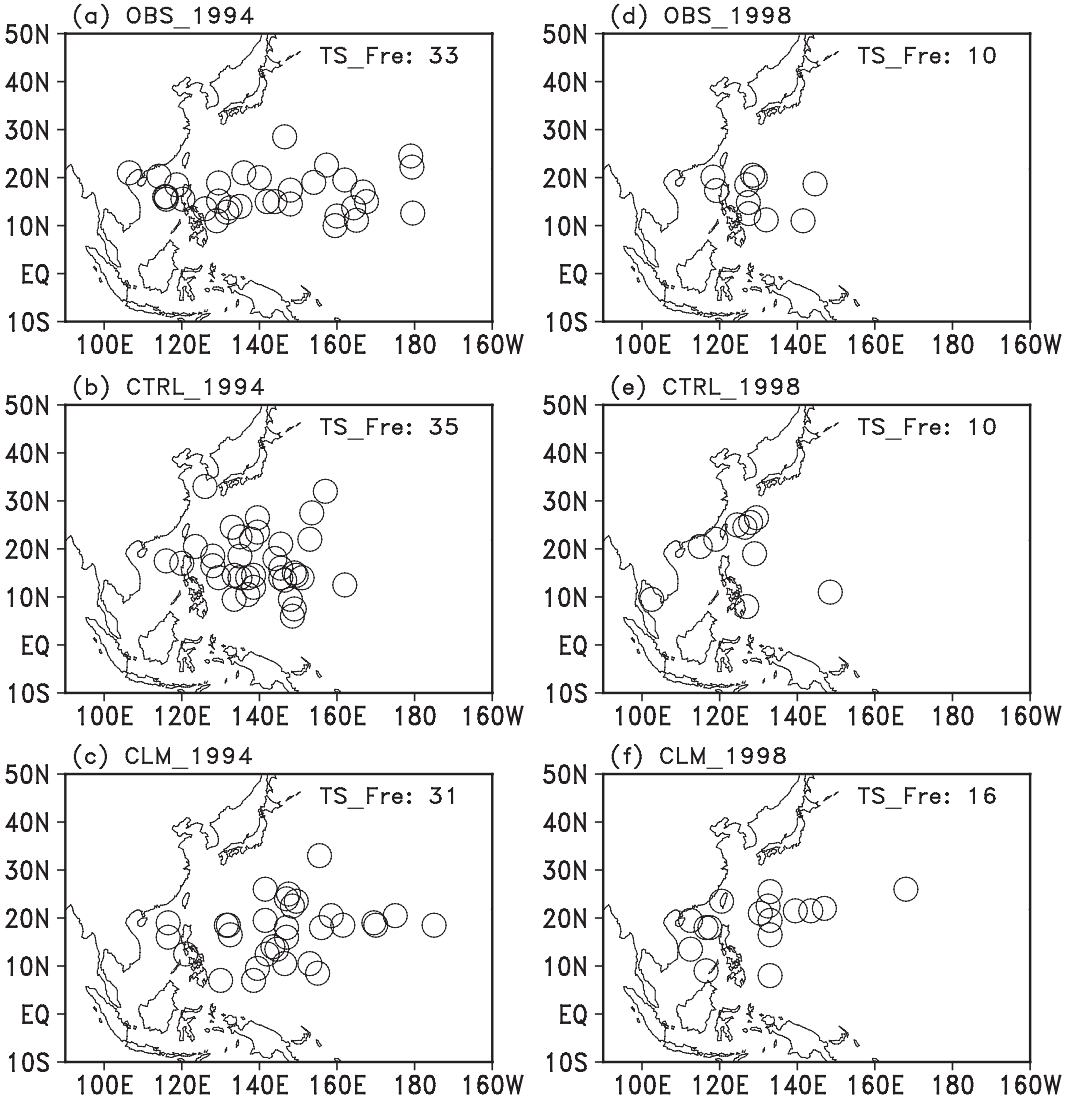

FIG. 10. As in Fig. 7, but in the typhoon seasons of (left) 1994 and (right) 1998 for (a),(d) the observations; (b),(e) the CTRL run; and (c),(f) the CLM run.

CTRL simulations and the observation is evident. In 1994, the TCs in the CTRL simulation form much more in the central WNP and less in the west WNP than in the observation, while the reverse bias pattern is simulated in 1998. After the EIO SST is replaced by climatology values, the TC frequencies in the three subregions increase in 1998, especially in the west and central WNP. In contrast, the change of TC frequency in 1994 is different in subregions, with a clear decrease in the central WNP and an increase in the east WNP, which leads to less change in total number of TC genesis. These results suggest that the model has the ability to reproduce some features of the TC genesis locations in extreme years, although the fidelity compared to that of the real world still need to be greatly improved. In addition, the sensitivity experiments further confirm that the EIO SSTA affects the TC genesis in the entire genesis region over the WNP, more importanty in the west and central WNP.

Figure 11 shows the mean 850-hPa wind fields for the typhoon season of 1998 from the NCEP–NCAR reanalysis and the model simulations and the difference of 850-hPa winds between the CTRL run and the CLM_1998 run. The CTRL run (Fig. 11b) captures the overall pattern of large-scale flow in the reanalysis well except for an deepening of the SCS summer monsoon trough and a slightly eastward shift of the WNP subtropical high. With the climatological mean SSTs in the EIO in 1998, the large-scale flow changes to a pattern more favorable for

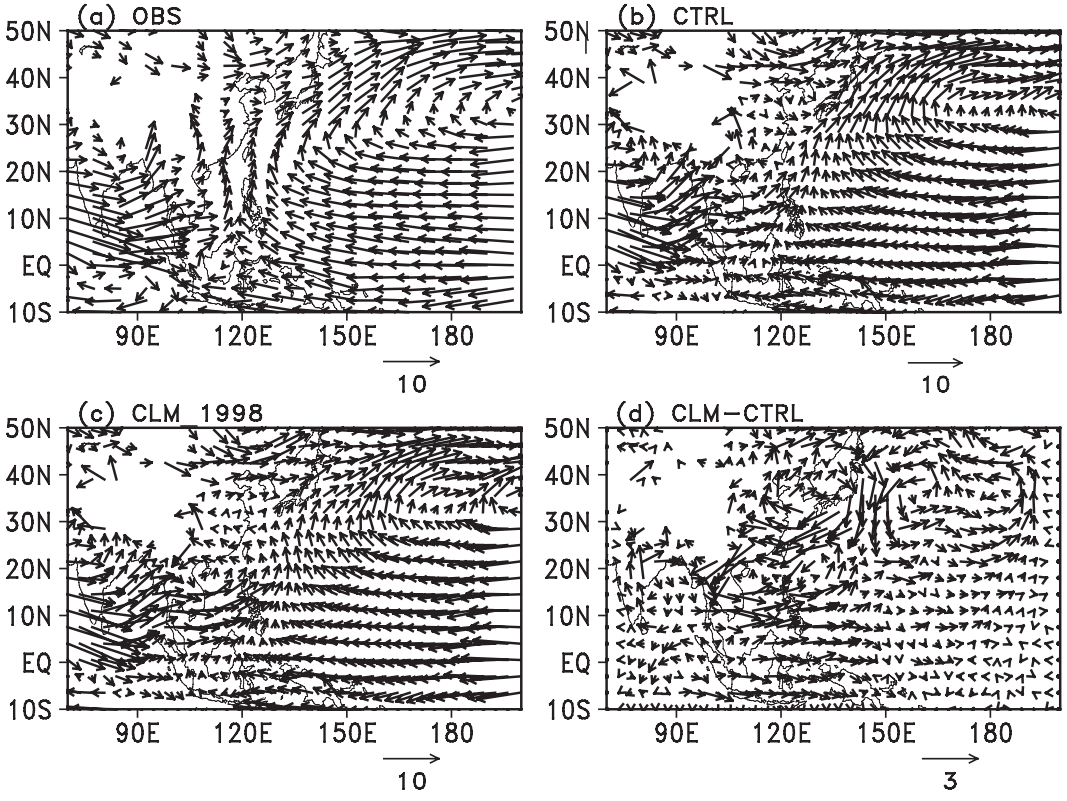

FIG. 11. 850-hPa wind fields averaged in the typhoon season of 1998 from (a) the NCEP–NCAR reanalysis, (b) the CTRL run, (c) the CLM_1998 run, and (d) the difference in 850-hPa winds between (c) and (b).

TC genesis over the WNP. This can be easily seen from the difference field in 850-hPa winds between the CTRL run and the CLM_1998 run (Fig. 11d). The anomalous southwesterly winds occur from the Indochina Peninsula to the WNP, and an anomalous cyclonic circulation appears over the SCS and the western WNP, collocated with the main WNP TC genesis region.

Figure 12 shows the vertical shear of zonal wind (which dominates the total vertical shear in the region) during the typhoon season of 1998 for the NCEP–NCAR reanalysis and the model simulation. A prominent feature is that the model captures the overall pattern of the vertical wind shear well (Figs. 12a,b). In particular, the features with a negative (positive) shear west (east) of 140°E and south (north) of about 25°N are presented well in the model. However, little model biases that are responsible for the few simulated TC formations to the northeast are also obvious. For example, the simulated easterly shear over the SCS is stronger than the observed. This might be because of the fact that the summer monsoon trough in that region is not well simulated as mentioned above. The low-shear region in the CTRL simulation unrealistically extends to the east of 150°E between 20° and 30°N. With the climatological mean SSTs in the EIO in 1998, the positive shear anomalies occur between 10° and 30°N and west of 150°E, namely, in the main WNP TC genesis region, suggesting a weaker vertical shear in that region than in the CTRL simulation. Therefore, changes in both the low-level circulation and the increased vertical shear associated with the positive EIO SSTA suppress TC genesis over the WNP, consistent with more TCs produced in the CLM_1998 run than in the CTRL run.

In sharp contrast, changes in the large-scale circulation in the CLM_1994 run from the CTRL run (not shown) are generally smaller than those for 1998 seen in Fig. 11d. This indicates that the EIO SSTA imposes a much weaker impact on the large-scale circulation in East Asia and WNP in 1994 than in 1998. In addition, changes in vertical shear associated with the EIO SSTA in the CLM_1994 run from the CTRL run (not shown) is favorable for TC genesis, partly offsetting the effect of low-level circulation. These changes account for only about a 10% decrease in the simulated TCs in the LCM_1994 from the CTRL run (Table 2). Therefore, the extremely high frequent TC activity in 1994 could be caused by factors other than the EIO SSTA and needs to be investigated in future studies.

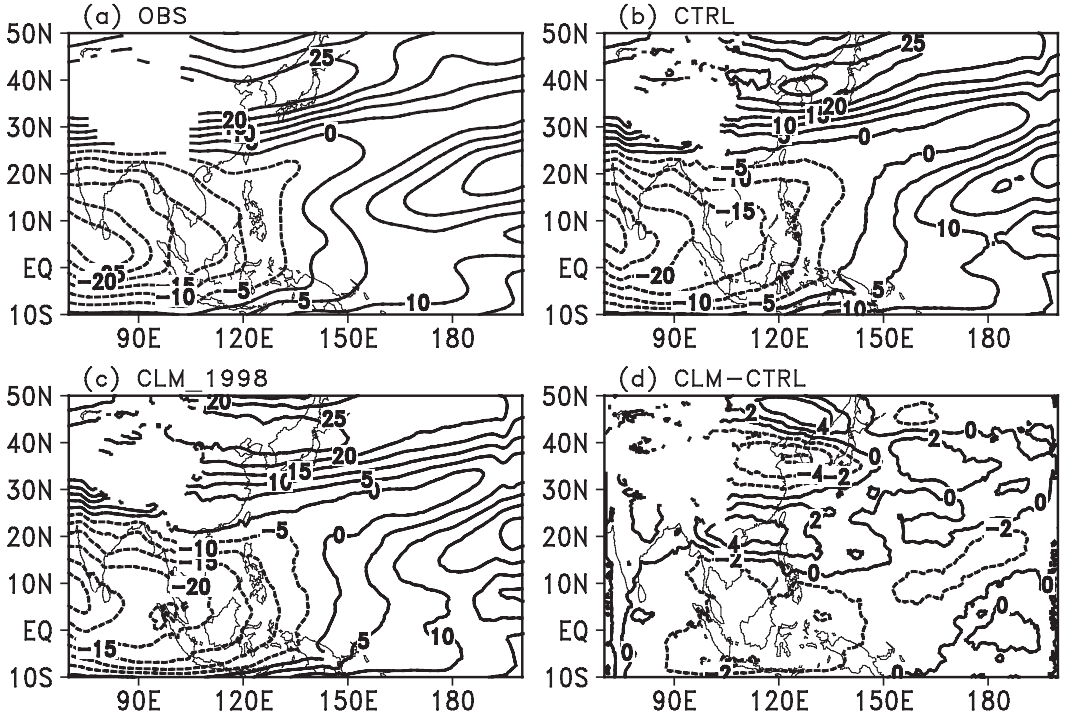

FIG. 12. As in Fig. 11, but for zonal wind vertical shear (in m s^{-1}) between 200 and 850 hPa.

5. Conclusions and discussion

a. Conclusions

In this study, the causal relationship between the EIO SSTA and the WNP TC frequency and the involved physical mechanisms proposed by Zhan et al. (2011) have been further examined using the IPRC Regional Atmospheric Model (iRAM), which was driven by the NCEP–NCAR reanalysis and the observed and modified SSTs. Our experiments consist of a 19 typhoon season control simulation with the observed SST and four sensitivity runs with either perturbed SST or with the observed SST replaced by the climatological SST in the EIO.

The control simulation reproduces realistically the observed variability of the WNP TC genesis frequency, including the seasonal and interannual variations and the trend since 1990. The geographical distributions of TC genesis and the frequency of occurrence over the WNP are also reasonably simulated. In addition, the observed statistical relationship between the WNP TC frequency and the EIO SSTA is well captured in the control simulation as well. Therefore, our results demonstrate that the model has significant skills in simulating the response of the WNP TC genesis to the EIO SSA. This urges us to use the model to further evaluate contributions of the EIO SSTA to the interannual variability of the WNP TC genesis frequency and changes in TC numbers in extremely high and low TC activity years in the studied period.

To evaluate the effect of the EIO SSTA on TC genesis over the WNP, we performed two perturbed SST runs for a normal year (2004) with negligible SSTA in the EIO. The results show that the TC number decreases by 32% in the perturbed run with the EIO 1°C warmer (WS_2004), and increases by 46% in the perturbed run with the EIO 1°C colder (CS_2004) than in their counterpart CTRL run. In the WS_2004 (CS_2004) run, warm (cold) EIO SSTA implies the reduced (enhanced) land–sea thermal contrast, leading to weaker (stronger) than normal SCS and WNP summer monsoon and its associated monsoon trough, thus suppressing (promoting) TC genesis over the WNP. In addition, the EIO warm (cold) SSTA can excite a warm (cold) equatorial Kelvin wave to the east, lowering (increasing) the surface pressure in the equatorial region and leading to anomalous anticyclonic (cyclonic) vorticity and divergence (convergence) in the lower troposphere in the tropics off the equator in the WNP TC genesis region. These dynamical conditions further suppress (promote) TC genesis over the WNP. The above results confirm the conceptual model proposed by Zhan et al. (2011) as schematically shown in Fig. 1.

Results from two climatological EIO SST runs for the extremely high and low WNP TC frequency years suggest

that the EIO SSTA can help explain and contribute to the unusual WNP TC frequencies in extreme years. The TC numbers in 1994 with the most TCs and in 1998 with the fewest TCs display a tendency toward the climatological mean value in the simulations with the EIO SST replaced by the climatological mean. However, the extent of the contribution varies greatly. Our results suggest that the warm EIO might be a major factor leading to the unusually few TCs formed over the WNP in 1998, but the cold EIO seemed to contribute little to the excessive WNP TCs in 1994. In other words, factors other than the EIO SSTA may contribute to the TC genesis in 1994 to a larger extent.

b. Discussion

There are some noticeable deficiencies in our simulations although the model generally demonstrates adequate skills in simulating the TC genesis frequency over the WNP. For example, the model failed to simulate the TCs as intense as the observed, a shortcoming common in this and previous studies with limited model resolutions. The genesis frequency of the WNP TCs has been underestimated after 2000 in the model, which leads to somewhat fewer total TC number for the 19 typhoon seasons in the control simulation than in the observation. The simulated mean TC frequencies in September and October are also lower than those observed. Nevertheless, the relations among the observed TC number, the simulated TC number during June and August, and EIO SSTA in summer are significant over the 90% confidence level based on the Student's *t* test. It suggests that this deficiency does not affect our conclusions. In addition, the simulated TC genesis locations seem to extend northward compared with observations, in particular for the region east of the Philippines. A point to keep in mind here is that the model with a 50-km resolution is employed in this study. The somewhat coarse resolution may have an influence on tracking/detecting TC-like vortices in the model. It is anticipated that these deficiencies could be alleviated by using a finer model resolution in the future. Furthermore, the finer resolution might also be useful in exploring other issues including future changes of the WNP TC activity as studied in Stowasser et al. (2007).

We have shown through sensitivity experiments that the EIO SSTA might contribute little to the excessive WNP TCs in 1994. To further verify the robustness of the results from single simulations presented in section 4, we conducted the ensemble simulations for 1994 with different initial conditions including seven control runs as in the CTRL run and seven sensitivity runs as in the CLM_94 run. They were initialized at 0000 UTC on 7 successive days from 21 to 27 May of each year and were run until 1800 UTC 31 October. Although the simulated TC frequencies for the typhoon season in 1994 show significant internal variability among the individual simulations, the ensemble means from the 7 control runs and the 7 sensitivity runs are, respectively, very similar to those of CTRL and CLM_94 discussed in section 4, with 31 TCs from the control runs and 29 from the sensitivity runs. In addition, 1994 recorded the third coldest EIO SST but the highest number of the WNP TCs in the period 1990–2008, which could not be explained only based on the EIO SSTA–WNP TC relationship. These results strongly suggest that factors other than the EIO SSTA may be dominant in determining the TC genesis in 1994. Our preliminary analysis shows a possible impact of the SSTA in the South Pacific east of Australia on the WNP TC activity in 1994, but more detailed analyses are needed to verify this assertion. Therefore, processes leading to the interannual variability of TC activity over the WNP deserve further investigation.

Acknowledgments. This study has been supported in part by the NSF Grant ATM-0754029 awarded to University of Hawaii and the NSFC Grants 40805040 and GYHY200806009. Additional support has been provided by the Japan Agency for Marine-Earth Science and Technology (JAMSTEC), NASA, and NOAA through their sponsorship of the International Pacific Research Center at the University of Hawaii at Manoa.

REFERENCES

Camargo, S. J., and A. H. Sobel, 2005: Western North Pacific tropical cyclone intensity and ENSO. *J. Climate,* **18,** 2996–3006.

——, H. L. Li, and L. Q. Sun, 2007: Feasibility study for downscaling seasonal tropical cyclone activity using the NCEP regional spectral model. *Int. J. Climatol.,* **27,** 311–325.

Chan, J. C. L., 2000: Tropical cyclone activity over the western North Pacific associated with El Niño and La Niña events. *J. Climate,* **13,** 2960–2972.

——, and K. S. Liu, 2001: Improvements in the seasonal forecasting of tropical cyclone activity over the western North Pacific. *Wea. Forecasting,* **16,** 491–498.

——, J. E. Shi, and C. M. Lam, 1998: Seasonal forecasting of tropical cyclone activity over the western North Pacific and the South China Sea. *Wea. Forecasting,* **13,** 997–1004.

Chen, T. C., S. Y. Wang, and M. C. Yen, 2006: Interannual variation of the tropical cyclone activity over the western North Pacific. *J. Climate,* **19,** 5709–5720.

Cheung, K. K. W., 2004: Large-scale environmental parameter associated with tropical cyclone formations in the western North Pacific. *J. Climate,* **17,** 466–484.

Chia, H. H., and C. F. Ropelewski, 2002: The interannual variability in the genesis location of tropical cyclones in the Northwest Pacific. *J. Climate,* **15,** 2934–2944.

Dickinson, R. E., A. Henderson-Sellers, and P. J. Kennedy, 1993: Biosphere–atmosphere transfer scheme (BATS) version 1e as

coupled to the NCAR Community Climate Model. NCAR Tech. Note NCAR/TN-387STR, National Center for Atmospheric Research, Boulder, CO, 72 pp.

Du, Y., L. Yang, and S. P. Xie, 2011: Tropical Indian Ocean influence on Northwest Pacific tropical cyclones in summer following strong El Niño. *J. Climate,* **24,** 315–322.

Edwards, J. M., and A. Slingo, 1996: Studies with a flexible new radiation code. I: Choosing a configuration for a large-scale model. *Quart. J. Roy. Meteor. Soc.,* **122,** 689–719.

Giorgi, F., M. R. Marinucci, G. T. Gates, and G. De Canio, 1993: Development of a second-generation regional climate model (RegCM2). Part II: Convective processes and assimilation of lateral boundary conditions. *Mon. Wea. Rev.,* **121,** 2814–2832.

Kalnay, E., and Coauthors, 1996: The NCEP/NCAR 40-Year Reanalysis Project. *Bull. Amer. Meteor. Soc.,* **77,** 437–471.

Knutson, T. R., R. E. Tuleya, and Y. Kurihara, 1998: Simulated increase of hurricane intensities in a CO_2-warmed climate. *Science,* **279,** 1018–1020.

——, J. J. Sirutis, S. T. Garner, I. M. Held, and R. E. Tuleya, 2007: Simulation of the recent multidecadal increase of Atlantic hurricane activity using an 18-km-grid regional model. *Bull. Amer. Meteor. Soc.,* **88,** 1549–1565.

——, ——, ——, G. A. Vecchi, and I. M. Held, 2008: Simulated reduction in Atlantic hurricane frequency under twenty-first-century warming conditions. *Nat. Geosci.,* **1,** 359–364, doi:10.1038/ngeo202.

——, and Coauthors, 2010: Tropical cyclones and climate change. *Nat. Geosci.,* **3,** 157–163, doi:10.1038/ngeo779.

Lander, M. A., 1994: An exploratory analysis of the relationship between tropical storm formation in the western North Pacific and ENSO. *Mon. Wea. Rev.,* **122,** 636–651.

Langland, R. H., and C. S. Liou, 1996: Implementation of an E–ε, parameterization of vertical subgrid-scale mixing in a regional model. *Mon. Wea. Rev.,* **124,** 905–918.

Liang, X., K. E. Kunkel, and A. N. Samel, 2001: Development of a regional climate model for U.S. Midwest applications. Part I: Sensitivity to buffer zone treatment. *J. Climate,* **14,** 4363–4378.

Murakami, H., B. Wang, and A. Kitoh, 2011: Future change of western North Pacific typhoons: Projections by a 20-km-mesh global atmospheric model. *J. Climate,* **24,** 1154–1169.

Nguyen, K. C., and K. J. E. Walsh, 2001: Interannual, decadal, and transient greenhouse simulation of tropical cyclone–like vortices in a regional climate model of the South Pacific. *J. Climate,* **14,** 3043–3054.

Philander, S. G. H., 1990: *El Niño, La Niña, and the Southern Oscillation*. Academic Press, 280 pp.

Ramage, C. S., and A. M. Hori, 1981: Meteorological aspects of El Niño. *Mon. Wea. Rev.,* **109,** 1827–1835.

Reynolds, R. W., N. A. Rayner, T. M. Smith, D. C. Stokes, and W. Wang, 2002: An improved in situ and satellite SST analysis for climate. *J. Climate,* **15,** 1609–1625.

Stowasser, M., Y. Wang, and K. P. Hamilton, 2007: Tropical cyclone changes in the western North Pacific in a global warming scenario. *J. Climate,* **20,** 2378–2396.

Sun, Z., and L. Rikus, 1999: Improved application of exponential sum fitting transmissions to inhomogeneous atmosphere. *J. Geophys. Res.,* **104,** 6291–6303.

Tiedtke, M., 1989: A comprehensive mass flux scheme for cumulus parameterization in large-scale models. *Mon. Wea. Rev.,* **117,** 1779–1800.

Vitart, F., and J. L. Anderson, 2001: Sensitivity of Atlantic tropical storm frequency to ENSO and interdecadal variability of SSTs in an ensemble of AGCM integrations. *J. Climate,* **14,** 533–545.

Wang, B., and J. C. L. Chan, 2002: How strong ENSO events affect tropical storm activity over the western North Pacific. *J. Climate,* **15,** 1643–1658.

Wang, Y., 1999: A triply nested movable mesh tropical cyclone model with explicit cloud microphysics—TCM3. BMRC Research Rep. 74, Bureau of Meteorology Research Centre, Melbourne, Australia, 81 pp.

——, 2001: An explicit simulation of tropical cyclones with a triply nested movable mesh primitive equation model: TCM3. Part I: Model description and control experiment. *Mon. Wea. Rev.,* **129,** 1370–1394.

——, O. L. Sen, and B. Wang, 2003: A highly resolved regional climate model (IPRC_RegCM) and its simulation of the 1998 severe precipitation events over China. Part I: Model description and verification of simulation. *J. Climate,* **16,** 1721–1738.

——, L. R. Leung, J. L. McGregor, D. K. Lee, W. C. Wang, Y. H. Ding, and F. Kimura, 2004a: Regional climate modeling: Progress, challenges and prospects. *J. Meteor. Soc. Japan,* **82,** 1599–1628.

——, S. P. Xie, H. M. Xu, and B. Wang, 2004b: Regional model simulations of marine boundary layer clouds over the Southeast Pacific off South America. Part I: Control experiment. *Mon. Wea. Rev.,* **132,** 274–296.

——, L. Zhou, and K. P. Hamilton, 2007: Effect of convective entrainment/detrainment on simulation of tropical precipitation diurnal cycle. *Mon. Wea. Rev.,* **135,** 567–585.

Xie, S. P., K. M. Hu, J. Hafner, H. Tokinaga, Y. Du, G. Huang, and T. Sampe, 2009: Indian Ocean capacitor effect on Indo–western Pacific climate during the summer following El Niño. *J. Climate,* **22,** 730–747.

Zhan, R., Y. Wang, and X. Lei, 2011: Contributions of ENSO and East Indian Ocean SSTA to the interannual variability of Northwest Pacific tropical cyclone frequency. *J. Climate,* **24,** 509–521.